Continuous chirality measures in transition metal chemistry

Santiago Alvarez,*[a] Pere Alemany[b] and David Avnir*[c]

Received 2nd November 2004
First published as an Advance Article on the web 11th February 2005
DOI: 10.1039/b301406c

The definition of the *continuous chirality measure* (CCM) is provided and its applications are summarized in this *tutorial review*, with special emphasis on the field of transition metal complexes. The CCM approach, developed in recent years, provides a quantitative parameter that evaluates the degree of chirality of a given molecule. Many quantitative structural correlations with chirality have been identified for most of the important families of metal complexes. Our recent research has shown that one can associate the chirality measures with, *e.g.*, enantioselectivity in asymmetric catalysis. We also explore a fragment approach to chirality in which we investigate which part of a molecule is responsible for the chirality-associated properties of a given family of compounds.

1. Continuous chirality measures: the concept

Chirality is such a central concept in chemistry and biochemistry, linked to problems which range from the origin of life to modern drugs, that one wonders why its descriptive language is so dull: A molecule is either chiral or not. The awkwardness of this limited language is immediately evident by considering the following series of substituted 2-butanes (see **1**): 2-fluorobutane and 2-iodobutane are of course chiral, but so is 2-deuteriobutane, which is only marginally different from the parent achiral butane. The intuition of the reader probably dictates correctly that since the 2-deuterio derivative is actually not that different from the achiral n-butane, its "degree of chirality" is quite small. Likewise the reader may feel that iodobutane is perhaps "more chiral" than fluorobutane, because the iodine atom is much larger than the fluorine atom, and therefore disturbs more the achirality of butane. Increasing even more the 2-substituent, one can perhaps say that 2-phenylbutane is "highly chiral", but if the very large coronene is used as a substituent, then the chirality of 2-coronenobutane is not so pronounced, because the butyl substituent on the very large polycyclic molecule is just a small disturbance to its achirality.

*santiago@qi.ub.es (Santiago Alvarez)
david@chem.ch.huji.ac.il (David Avnir)

Santiago Alvarez

Santiago Alvarez was born in Panamá, República de Panamá in 1950. He studied Chemistry at the University of Barcelona, where he obtained a PhD working on vibrational spectroscopy with Professor Jaume Casabó. After doing experimental research on one dimensional conductors in Barcelona, he carried out theoretical research at Cornell University with Professor Roald Hoffmann in 1983–1984. He returned to Barcelona where he was appointed as Professor Titular in 1984 and as Catedrático (Professor) in 1987. His research has been focused since on the theoretical study of bonding and structure in transition metal compounds, both molecules and extended solids, and on the correlation between molecular or crystal structure and physical properties. Recently he became interested in the application of continuous symmetry and shape measures to the stereochemical description of transition metal compounds.

Pere Alemany

Pere Alemany i Cahner was born in Barcelona, Spain in 1962 and graduated in Chemistry in 1986 at the University of Barcelona. In 1987 he joined the group of Professor S. Alvarez at the University of Barcelona to obtain his doctorate in 1991. In 1992 he carried out postdoctoral work with Professor Roald Hoffmann at Cornell University, USA working on theoretical aspects of metal–ceramic interfaces. In 1993 he joined the Physical Chemistry Department of the University of Barcelona as Assistant Professor. He assumed his current position as Associate Professor at the same institution in 1997. His research interests are mainly centered in the electronic structure of inorganic solids and the development and application of continuous symmetry measures to problems of structural chemistry.

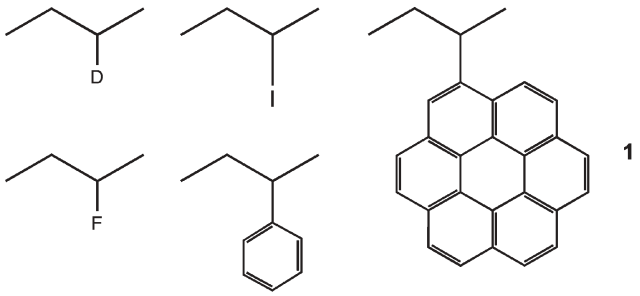

1

This intuition follows in other families: the amino acids, the helicenes, the bis-chelated four coordinated metal complexes, are some representative examples. Quantifying this intuition into a scale of chirality, *i.e.*, being able to tell by how much one molecule is more chiral than another, opens for chemists the ability to ask a new type of questions that enriches the arsenal of structural chemistry. Here are some examples:

* What is the continuous change in the level of chirality of a molecule as it rotates or vibrates?

* Is there a correlation between the degree of chirality of a homologous series of catalysts and the resulting enantiomeric excess of the reaction product?

* Is there a correlation between the degree of chirality of a series of enzyme inhibitors and the efficiency with which they inhibit that enzyme?

* Is there a correlation between the enantiomeric separation efficiency of a chiral chromatographic column and the degree of chirality of the separated enantiomers?

* Can quantitative chirality be used as a reaction coordinate? How does energy vary with chirality?

* How does the degree of chirality of a chiral crystal change as pressure is applied? And how about the temperature effects on chirality?

* How does optical rotation change with chirality?

* Can one identify a correlation between chirality and magnetic moments?

The aim of this brief review is to draw attention to the fact that, *yes, today it is possible to answer these and many other related questions in the realm of chirality*. Many propositions as to how to measure chirality have appeared in the literature (for comprehensive reviews with extensive listings of contributions to the field of chirality measures, see refs. 1 and 2). Here we concentrate on the method we have developed in recent years,[2,3] which offers the following advantages:

(a) It treats the measurement of chirality in the more general framework of measurement of symmetry. The Continuous Symmetry Measure (CSM) described below provides a general approach for the evaluation of the degree of content of *any* symmetry point group, and puts all the specific measures on the same quantitative scale. Thus, the continuous chirality measure (CCM) consists of measuring the deviation of the structure of the studied molecule from having an achiral point group. A whole stereochemical symmetry/chirality profile is then provided. For instance, for a four-coordinated species, one can obtain the degree of tetrahedricity, of C_{3v}-ness, of C_{2v}-ness, of the rotational symmetries (*e.g.*, the degree of being C_3), and of chirality, namely (in this case), of minimal distance of the molecule to a (hypothetical) structure which has a mirror symmetry (not necessarily a C_{nv} structure). In this brief review we concentrate only on the latter.

(b) Of the various proposed chirality measurement tools, the one described here proved to be the most versatile. It is the only method with which answers to *all* of the above listed questions—and many more—were provided (see refs. 4,5 and earlier references cited therein). Some of these answers are presented in this review, as representative of the whole approach.

(c) The identified correlations between the chirality measure and various chemical, biochemical or physical measurables that depend on it, translate the qualitative links that were known before the measure was applied into quantitative descriptions that follow and expand faithfully those qualitative descriptions.

David Avnir

David Avnir is currently interested in sol–gel materials, in composite metallic materials, and in theoretical and computational aspects of symmetry and chirality. Earlier major interests included fractal theory and far-from-equilibrium phenomena. Five of his papers are on the ISI list of the 200 most cited chemistry publications for the period 1982–2001.

2. Continuous symmetry and chirality measures: the methodology

The evaluation of the chirality content of an object by the CCM approach requires finding the nearest structure that is achiral. Thus, it is a function of the minimal distance that the vertices of the object (the molecule's nuclei) have to be shifted in order to attain the desired achiral symmetry. Formally, given a (chiral) structure Q composed of N vertices whose $3N$ cartesian coordinates q_k are arranged in N vectors $\vec{q}_i$, one searches for the coordinates of the nearest perfectly G-symmetric object (G being the nearest achiral symmetry group), whose cartesian coordinates p_k are contained in N vectors $\vec{p}_i$. Once at hand, the symmetry measure of Q with respect to G is defined as

$$S_Q(G) = \min \left[\frac{\sum_{i=1}^{N} |\vec{q}_i - \vec{p}_i|^2}{\sum_{i=1}^{N} |\vec{q}_i - \vec{q}_0|^2} \right] \times 100 \qquad (1)$$

In eqn. (1), $\vec{q}_o$ is the position vector of the geometric center of the analyzed structure Q, and the denominator is a mean square size normalization factor. The bounds are $0 \leqslant S \leqslant 100$: if a structure has the desired (achiral) G-symmetry, then $S(G) = 0$ and the symmetry measure increases as it departs from G-symmetry (increase in chirality), reaching a maximal value (not necessarily 100). The same procedure can be applied to determine the

proximity of a molecular structure to a given symmetry point group, and we talk then of the *continuous symmetry measures* (CSM). All $S(G)$ values, regardless of G or of the structure, are on the same scale and therefore comparable: One can thus compare the degree of, say, perfect octahedricity (O_h-ness), D_{4h}-ness or chirality ($S(C_s)$) of various distorted ML_6 molecules;[6] one can compare the chirality of molecules with different number of ligands; or one can compare different symmetry contents of different molecules.

The main computational task is to find the nearest structure that has the desired symmetry, namely to minimize eqn. (1) in order to get $\{p_k, k = 1, 2\ldots 3N\}$. Several methods, both general and problem-specific, have been developed towards this goal, and are described in the literature.[7,8] It should be noted again that the determination of the degree of chirality (the nearest achiral symmetry point group content) means searching for the nearest achiral structure which, in the simplest case, may have one reflection plane. In this case $S(G_{achiral}) = S(C_s)$, and the nearest achiral point group is composed of the reflection and identity elements. For instance, the nearest achiral structure to a helix is a plane onto which the helix points have been collapsed.[9] However, the nearest achiral structure may contain more than one mirror plane and the achirality of the nearest structure need not be based on a mirror plane, but may have its origin in other improper symmetry elements (any of the S_n elements, n being an even integer). We can also distinguish between structural and substitutional chirality. The former is associated with the geometric disposition of the atoms regardless of their chemical nature, whereas the latter takes into consideration the inequivalence of different chemical elements even if they may appear as mirror images of each other in a given molecule. As an example, an asymmetric $CR^1R^2R^3R^4$ molecule may be structurally achiral (but chemically chiral) if all C-R^i bonds have the same lengths and all R^i–C–R^j bond angles are tetrahedral. We shall be concerned in this review mostly with structural chirality. Although such an approach may seem naïve at first sight, size and electronegativity differences are reflected in bond distances and angles, which allows us to differentiate different degrees of chirality between, *e.g.*, the fluoro- and iodo- substituted butane shown in **1**. More rigorous measures of chemical chirality should analyze the degree of chirality of the electron density, a matter that is currently under investigation by us and by Bellarosa and Zerbetto.[10]

3. Molecular chirality and shell chirality

If we wish to extract general ideas about the chirality behavior of transition metal complexes, we need to adopt some idealization that could be applied equally well to a wide variety of molecules differing in the topology of their ligands or on their substituents. To that end, we have found it useful to consider a molecule as formed by successive shells, as exemplified in **2** for the case of tris(dithiolene) complexes. The first shell comprises the metal and the coordinated donor atoms (*i.e.*, the coordination sphere), the second shell is formed by the spacers that connect each pair of donor atoms in a bidentate ligand, and the third shell is formed by the rest of the ligand atoms, typically substituents providing diverse inductive, steric or intermolecular bonding effects. Thus, we shall refer to the chirality measures as S_1 (that of first shell only), S_2 (second shell only), S_{1+2} (first and second shells together) and S_f for that of the full molecule (usually neglecting the hydrogen atoms that are not always well located in crystallographic studies). We shall see that in some cases the chirality of the first two shells combined bears some relationship to that of one of those shells only, and also that the chirality of the whole molecule may be related to S_1, S_2 or S_{1+2}. However, the reader must be warned that the shell chirality measures are in general not additive, *i.e.*, $S_{1+2} \neq S_1 + S_2$. Let us now proceed to show how the chirality analysis by shells can be applied to several families of transition metal compounds.

Homoleptic hexacoordinate complexes

We have shown[11] that a variety of hexacoordinate ML_6 complexes with monodentate ligands (notably alkyl, aryl and thiolato derivatives of metals with d^0 to d^2 electron configurations) have twisted geometries in their first shell (**3**), intermediate between the octahedron and the trigonal prism. At the two extremes of that path one has either an octahedron ($\theta_1 = 60^\circ$) or a perfect trigonal prism ($\theta_1 = 0^\circ$, D_{3h} symmetry, all edges equal to each other), both achiral structures. In-between ($0 < \theta_1 < 60^\circ$), the molecular symmetry is lowered to D_3 and the twisted structures are therefore chiral. On the CCM scale, the outcome is that, while the S value of the MX_6 group is zero for the two ideal polyhedra, in-between it has non-zero values for intermediate twist angles and should pass through at least one maximum. The S_1 line in Fig. 1 shows the computational expectation for a model of this twist route and it is seen that, indeed, a maximum chirality value appears

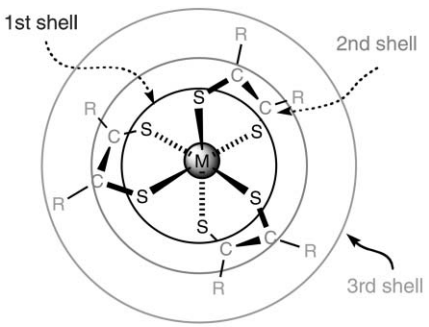

2

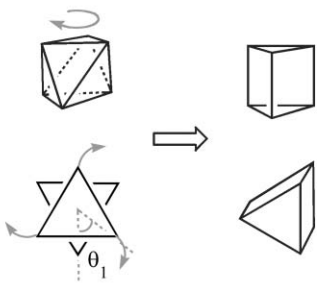

3

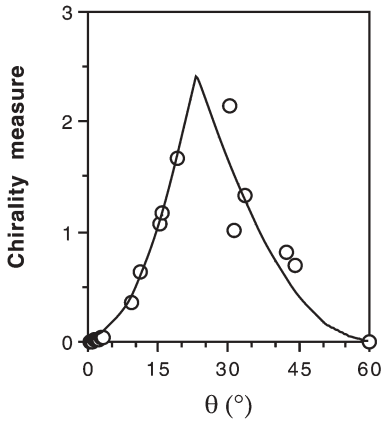

Fig. 1 Chirality measure for a model MX_6 molecule (continuous line) along the Bailar trigonal twist (see **3**). The experimental chirality measures of hepta-atomic MX_6 cores of homoleptic organometallic and thiolato complexes are shown as circles. Reproduced with permission from ref. 11. Copyright (2001) Wiley-VCH.

at $\theta_1 = 23^\circ$. Experimental data for alkyl, aryl and thiolato homoleptic complexes, also represented in Fig. 1, nicely follow the expected behavior. From that plot, we have identified several previously unnoticed chiral ML_6 complexes, among which the most chiral one,[12] $[Zr(SC_6H_4\text{-}4\text{-}OMe)_6]^{2-}$, has been predicted by a theoretical study to present a substantial barrier to enantiomerization.[13] We note that the reference achiral structure according to the CCM methodology is not necessarily the same throughout the pathway and for the different shells. Thus, it has been found that the cusp in the S_1 curve (Fig. 1) is associated to the fact that the closest achiral structure for $\theta_1 < 23^\circ$ is a trigonal prism, whereas the closest achiral geometry for larger rotation angles is a distorted octahedron with C_{2v} symmetry.

Tris(chelate) complexes

The first shell of the tris(chelate) complexes behaves exactly in the same way[14] as that of the systems with monodentate ligands, indicating that chirality is a common feature of Bailar-twisted molecules regardless of the denticity of their ligands. This result is in sharp contrast with the accepted view that attributes chirality in tris(chelate) complexes exclusively to the helical arrangement of the three chelate rings (*i.e.*, the second shell). Yet the arrangement of such rings presents helicity (hence chirality), so we should ask ourselves whether the chiralities of the first and second shells in tris(chelate) systems are correlated in some way or not.

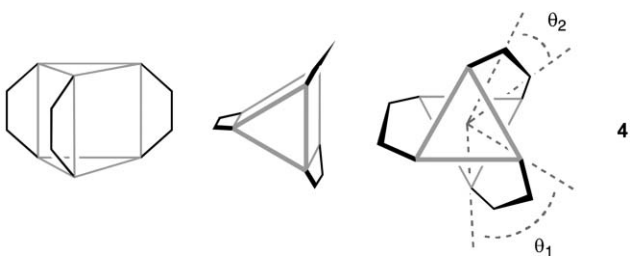

4

When a tris(chelate) complex is subject to a rotation around its trigonal axis, the backbones of the bidentate ligands follow that rotation. If the chelate rings are planar, as happens in dithiolates, bipyridine, phenanthroline, β-diketonates, dithiocarbamates and many other ligands, their behavior as a function of the rotation angle of the first shell, θ_1, is easily predictable. Thus, in the trigonal prismatic conformation ($\theta_1 = 0^\circ$), the chelate rings are placed at the symmetry planes that contain the trigonal axis (see **4**, left and center), a situation that is reflected in the angle formed by the projection of the atoms of the second shell onto a plane perpendicular to the trigonal axis ($\theta_2 = 0^\circ$). In summary, for a trigonal prismatic tris(planar-chelate) complex we expect the chirality measures of the first two shells, both independently or combined, to be zero: $S_1 = S_2 = S_{1+2} = 0$. When the first shell reaches the achiral octahedron ($\theta_1 = 60^\circ$), though, the second shell has still a much smaller rotation angle (θ_2 between 15 and 30° for several ligands analyzed), as schematically shown in **4** (right). As a consequence, the chirality of the second shell increases continuously from zero at $\theta_1 = 0^\circ$ up to 60° (Fig. 2).

As noted above for the homoleptic hexacoordinate complexes, the cusp in the S_1 curve (Fig. 2) is associated with the fact that the closest achiral structure for the first shell is different at small rotation angles ($\theta_1 < 23^\circ$) than at larger angles. In contrast, for the second shell, as well as for the combination of first and second shells, the closest achiral structure is a trigonal prism all the way between $\theta_1 = 0$ and $\theta_1 = 60^\circ$. We say that the chirality measures S_2 and S_{1+2} are commensurate with S_1 for $\theta_1 \leqslant 23^\circ$, but incommensurate for $\theta_1 > 23^\circ$, to indicate that chirality measures refer to the same or different achiral structures, respectively. Chirality measures are expected to be correlated only if they are commensurate, therefore, we can take S_1 for tris(chelate) complexes as an indication of the trends in S_2 and S_{1+2} only in the commensurate region ($\theta_1 \leqslant 23^\circ$).

We can go back now to a fundamental question and ask, which shell is responsible for the chirality of tris(chelate) complexes, the first or the second shell? The answer is: it depends on the twist angle. For complexes with twist angles θ_1

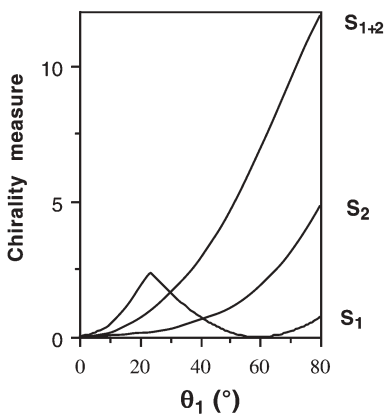

Fig. 2 Chirality measures as a function of the twist angle (see **3**) for a model tris(chelate) complex $M(S_2C_2)_3$. Shown are the chirality variation of the first shell S_1 (defined in **2**); that of the second shell, S_2, and that of the first and second shells combined, S_{1+2}. Adapted from ref. 14, Copyright (2001), with permission from Elsevier.

$< 23^\circ$, the largest contribution to chirality comes from the first shell. In the specific case of $\theta_1 = 60^\circ$, the first shell is achiral and chirality is due only to the helical conformation of the chelate rings (second shell), therefore at twist angles θ_1 slightly under 60° the main contribution comes from the second shell. However, for intermediate angles, both the first and second shell contribute significantly to molecular chirality.

Bis(chelate) complexes[15]

As opposed to hexacoordinate complexes, tetracoordinate ones are chiral when distorted from square planar to tetrahedral (or *vice versa*) only in the bis(chelate) families, but not when all ligands are monodentate. The reason is that in the presence of monodentate ligands, the interconversion between tetrahedron and square proceeds through the *spread* pathway, in which all metal-centered bond angles change along the path, giving intermediate structures of D_{2d} symmetry (**5**). On the other hand, a bidentate ligand imposes a practically constant chelate angle α, irrespective of the orientation of the ligands around the metal, making it different from the interligand bond angle β, and resulting in a chiral D_2 symmetry (**6**) along the whole of the *twist* pathway, except for the end points.

As in the tris(chelate) case, the chirality measure of the first shell in bis(chelate) complexes is not always commensurate with those of the second shell or of the first two shells combined, and the incommensurability has been seen to depend both on the bite angle of the bidentate ligand and the torsion angle between the two chelate rings ($\tau = 0$ and 90° for a square planar and a tetrahedral complex, respectively), and is illustrated in Fig. 3.

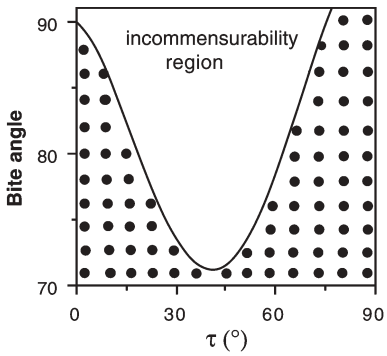

Fig. 3 Combinations of bite and torsion angles that result in commensurate (shaded region) and incommensurate (white region) S_1 and S_{1+2} values in bis(chelate) complexes. Reproduced from ref.15 with permission of the Royal Society of Chemistry.

Other chiral complexes

We have just seen that a perfectly octahedral (achiral) coordination sphere ($\theta = 60^\circ$) with achiral bidentate ligands may lead to a helical arrangement of the ligands, resulting in chiral complexes such as $[M(bipy)_3]$, even if neither the metal coordination sphere nor the individual chelate rings are chiral. There are other cases of chiral molecular topologies due to, *e.g.*, conformational helicity of the chelate rings or of the ligands themselves, and whose chiro-optical properties have not always received enough attention. We therefore briefly comment in this section on three additional families of chiral complexes: (a) the metaprismatic octacoordinate complexes (*i.e.*, those having geometries intermediate between the square antiprism and the cube), (b) the square planar propellers and

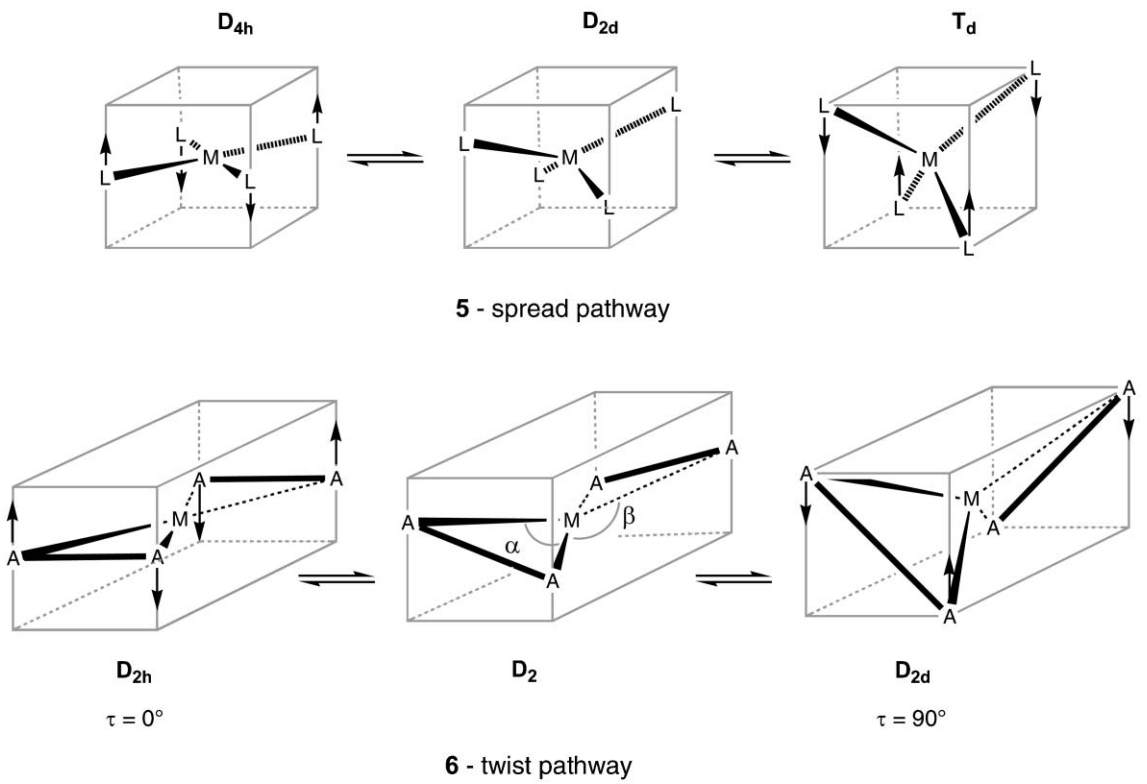

(c) the helices formed by tripod ligands.

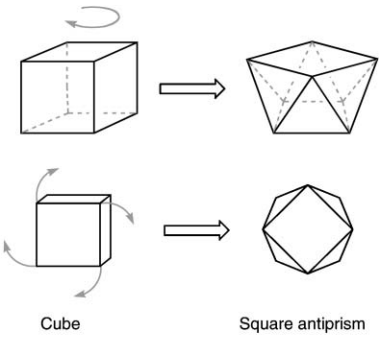

7

Metaprismatic octacoordinate geometries intermediate between the cube and the square antiprism can be obtained by rotating two parallel faces of a cube around a fourfold axis (**7**), in much the same way that the Bailar twist generates geometries in-between the octahedron and the trigonal prism. Since the interconversion of cube and square antiprism (both achiral structures) proceeds through the metaprismatic structures of D_4 symmetry, that are perforce chiral, a maximum chirality similar to those found in Figs. 1 and 2 should be expected. The calculation of the degree of deviation from the cube-square antiprism interconversion path[16] has allowed us to detect a family of complexes with calixarene-based octadentate ligands that present this type of chiral geometries.[17] It is interesting to establish a connection here with the coordination sphere of the divalent cations in the garnet structure, that is also metaprismatic and chiral.[16]

There is a family of square planar complexes with ligands that hinder the rotation around the metal–ligand bond and appear in propeller conformations, schematically depicted in **8**. The paradigmatic case is probably that of the tetra(aryl) complexes with bulky substituents at the *ortho* positions, such as C_6Cl_5. In such complexes, an achiral conformation with the aryl groups perpendicular to the coordination plane (rotation angle $\tau = 0^\circ$) would take the *ortho* chloro substituents to close proximity (about 2.7 Å), whereas in the experimental chiral conformation ($20^\circ < \tau < 29^\circ$ in a variety of $[M(C_6Cl_5)_4]$ complexes of Cr^{II}, Rh^{II}, Ir^{II}, Ni^{III}, Pt^{II}, Pt^{III} and Au^{III}), that distance is increased up to 3.3 Å. Since intramolecular enantiomerization requires approaching the *o*-chloro substituents, it seems likely that strong Cl···Cl steric repulsions would impose a high energy barrier to the enantiomerization (in a structural database search we found all intermolecular Cl···Cl contacts between aromatic molecules at distances larger than 3.00 Å). Therefore, enantiomerically pure samples of these anionic complexes could probably be isolated from solution through appropriate choice of chiral countercations. The Cr^{II} helix prepared by Forniés *et al.*[18] is a particularly intriguing case, since it crystallizes in the enantiomorphic I_4 space group and each single crystal should therefore be enantiomerically pure.

The third case of conformational helicity can be found in complexes with tripod ligands. Such ligands present a helical conformation in a number of penta- and tetracoordinate complexes, as schematically shown in **9**, in a projection down the trigonal axis, and many crystallize in enantiomorphic space groups. The fact that ligand coordination/dissociation in these complexes should be facile given the little reorganization of the coordination sphere required would make this family of chiral compounds interesting as potential enantioselective catalysts. However, it is likely that the chelate ring inversion that interconverts the two enantiomers **9** has a low activation energy and racemization may occur in solution.

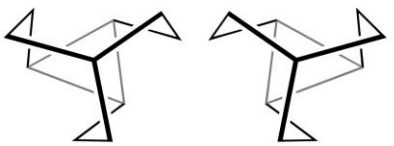

9

Chirality amplification and attenuation

From the chirality measures of the innermost shells of complexes we can in principle predict the chiral behavior of a wide variety of related molecules with a common coordination sphere but which differ in substituents or substitution patterns. But to do that we must be sure that the chirality measure of the inner shells gives a reasonable estimate of that of the full molecule. What we have found is that the chirality measure of the full molecule S_f (devoid of hydrogen atoms) shows a linear correlation with S_{1+2} within a family of complexes having analogous bidentate ligands, both for bis- and tris(chelate) complexes studied (Fig. 4). Closer inspection of those figures tells us that bidentate ligands can be classified in two categories, depending on whether there is chirality amplification (*i.e.*, S_f is always larger than S_{1+2}) or a chirality attenuation effect (S_f is always smaller than S_{1+2}). Specifically, it is seen that (i) the catecholato and dithiolene complexes obey the same relationship between the two chirality measures; (ii) in the cases of dithiolene, catecholato and dithiocarbamato

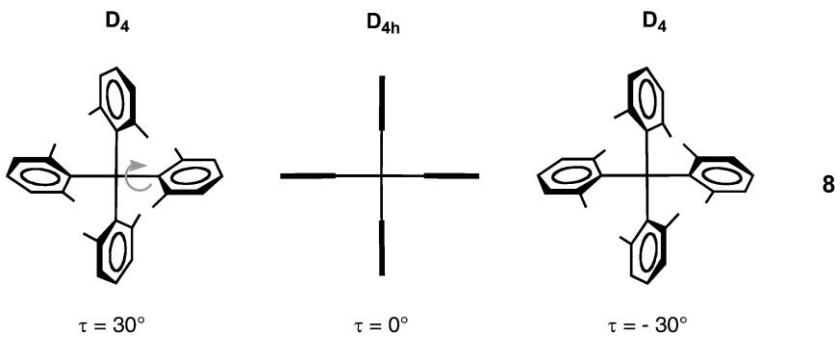

8

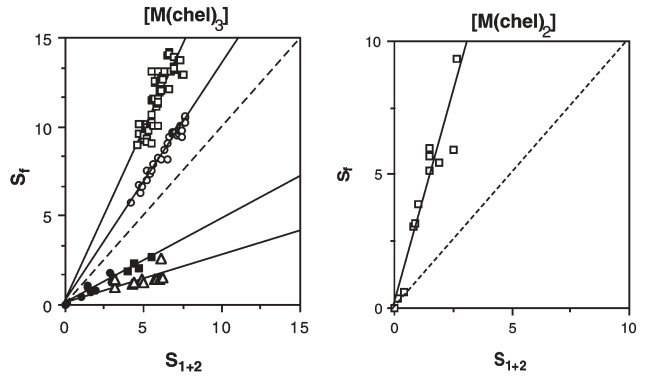

Fig. 4 Chirality measures of the full molecules (without hydrogen atoms), S_f, for families of tris- and bis(chelate) complexes as a function of S_{1+2}. The chelating ligands are: bipyridine or phenanthroline (open squares), β-diketonates (open circles), dithiolenes (filled circles), catecholates (filled squares) and dithiocarbamates (open triangles). The continuous lines are least-squares fittings of the experimental data; the dashed lines correspond to the ideal cases with $S_f = S_{1+2}$. Adapted from ref. 14, Copyright (2001), with permission from Elsevier, and from ref.15 with permission of the Royal Society of Chemistry.

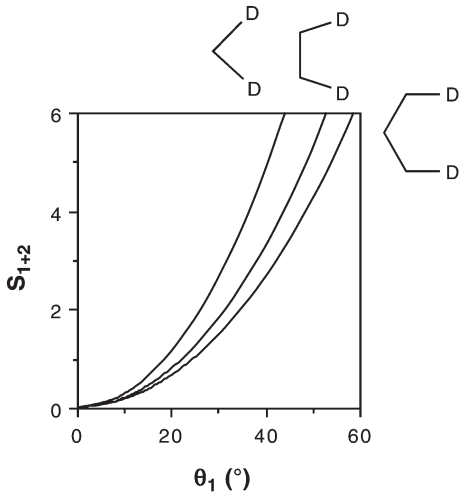

Fig. 5 Effect of the number of spacers of the bidentate ligands on the S_{1+2} chirality measures for tris(chelate) complexes with planar chelate rings, as calculated for model complexes. The same behavior has been found among the experimental structures of several families of tris(chelate) complexes. Adapted from ref. 14, Copyright (2001), with permission from Elsevier.

complexes, S_f is always smaller than S_{1+2}, and (iii) for the cases of bipyridine and β-diketonato complexes S_f is always larger than S_{1+2}.

In summary, the chirality measures of the first two shells combined reproduce the trend of the full molecular chirality within a family of complexes with related ligands. Two types of correlations can be found: for some families the chirality of the inner shells is amplified by the outer shells, whereas for other families the addition of the outer shells results in chirality attenuation. Since the first and second shell combined constitute the smallest fragment of tris(chelate) complexes that allows us to evaluate the chirality of the full complex, it is worth stressing the factors that seem to affect the value of S_{1+2}.

(a) S_{1+2} increases with the rotation angle θ_1 between two trigonal faces (**3**), as seen in Fig. 2. There, structures resulting from Bailar twists of the octahedron ($\theta_1 = 60°$) are not equivalent for clockwise ($\theta_1 < 60°$, see **10**, where the thicker line represents a bidentate ligand) and anticlockwise ($\theta_1 > 60°$) rotations. A clockwise rotation would ultimately lead to a prismatic geometry ($\theta_1 = 0°$) in which the bidentate ligands span edges of the trigonal prism, whereas an anticlockwise rotation takes us to a structure with the bidentate ligands occupying diagonals of the square faces of the trigonal prism.

(b) For the same degree of rotation, it can be seen that S_{1+2} decreases with increasing number of spacer atoms (Fig. 5).

(c) Since it has been shown that the rotation angle in tris(chelate) complexes increases with the normalized bite of the bidentate ligand,[19,20] the value of S_{1+2} increases with the normalized bite for ligands with the same number of spacer atoms (defined as the ratio between the donor–donor and the metal–donor distances in a chelate ring, **11**).

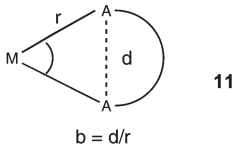

11

Ligand-centered chirality

The Cu(II) bisoxazoline complexes, widely used as catalysts for a variety of reactions, provide a nice illustration of how quantitative chirality measures may correlate with important chemical properties such as the enantiomeric excess of the catalyzed reactions and provides new insight into the stereochemistry of catalytically active transition metal complexes. First, it was found[21] that chirality measures of the full theoretically optimized structures of a family of complexes **12**, that differ only in the number of methylene groups forming the spirocycle at the bridgehead carbon atom, are well correlated to the experimental enantiomeric excess in the Diels–Alder reaction that they catalyze. Later on, a more detailed analysis[22] of shell chirality measures showed that the chirality of the full molecule is essentially determined by that of the fragment whose atomic symbols are shown in **13**, as seen

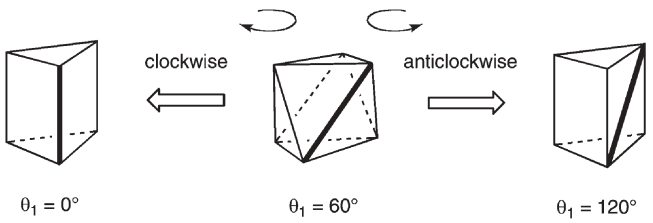

10

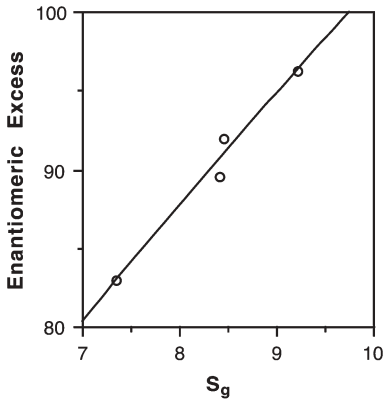

Fig. 6 Enantiomeric excess of a Diels–Alder reaction catalyzed by Cu bisoxazoline complexes **12** as a function of the chirality measure of the molecular fragment **13**. Reproduced with permission from ref. 22. Copyright (2003) Wiley-VCH.

in Fig. 6, where the corresponding enantiomeric excesses are represented as a function of the chirality measure of such fragment for each of the four bisoxazolines analyzed. An interesting paradox is that the changes in chirality of the different complexes analyzed are due to the different size of the spirocyclic group, whereas all the chirality information is contained in a molecular fragment **13** that does not include such a group. The explanation for such a paradox is that changes in the size of the spirocycle modify the CCC bond angle of the chelate ring and the position of the two carbonated flaps, thus affecting the position of the hydrogen atom at the α asymmetric carbon directly bonded to N. That hydrogen atom forms a weak C–H···O hydrogen bond with the triflate ligand and modifies in turn the position of such a group. In effect, it is the achiral spirocycle that tunes the chirality of the asymmetric portion of the molecule. Although the triflate ions do not participate in the catalytic reactions, it is likely that the asymmetry imposed to the reactants that coordinate to these sites is not different from that presented by these leaving groups.

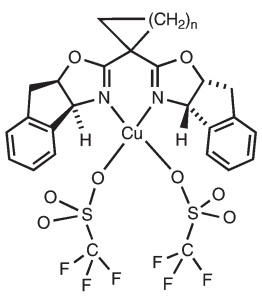

12

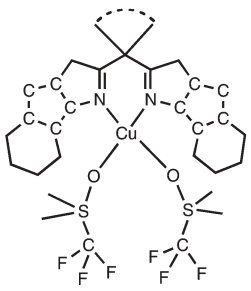

13

4. Chirality and racemization pathways

One of the most intriguing findings that result from the application of the continuous symmetry measures to the quantification of chirality arises when monitoring how the chirality of a dissymetric molecule changes along an enantiomerization path. Contrary to common intuition, the interconversion of left- and right-handed enantiomers of a molecule need not go through an achiral transition state. This property of the enantiomerization pathways, which has been known[23] long before the introduction of continuous chirality measures, allows us to classify the enantiomerization paths into two categories: achiral pathways (*i.e.* those paths which reach at some point an achiral structure) and chiral pathways in which the CCM never drops to zero. In order to illustrate these concepts we will analyze in this section with some detail the general case of enantiomerization processes through internal rotation and discuss three examples that represent different situations.

Internal rotation pathways

Here we focus on the general case of a molecular system with at least D_n symmetry. Among the large variety of families of compounds that fit into that picture we can mention ethane, the $[M_2L_8]$ compounds with multiple metal–metal bonding,[24] the metallocenes $[MCp_2]$, the $[ML_6]$ complexes along the Bailar trigonal path **3**, the $[M(chelate)_2]$ complexes along the twist path **6**, the octacoordinate complexes along the cube-square antiprism path **7** and the square propellers **8**. In such systems, the atoms that are not sitting on the C_n symmetry axis are grouped in sets of $2n$ equivalent atoms, forming two n-gons, as illustrated in **3** for the case of an $[ML_6]$ complex. The atoms in each n-gon are related through the proper C_n rotation, whereas the two polygons are related through the C_2 rotations. Then, the chirality of each set of equivalent atoms is determined by the rotation angle between the two n-gons, θ, as in the case of the two triangles depicted in **3**.

As seen in the case of the hexacoordinate complexes above, there are specific values of the rotation angle θ that present high symmetry and thus achiral conformations. In particular, for $\theta = 2k\pi/n$ ($k = 0, 1, 2, ...$) the two n-gons are eclipsed forming a prism of D_{nh} symmetry or higher (*e.g.*, a cube for $n = 4$) and for $\theta = (2k + 1)\pi/n$ they form an antiprism of D_{nd} symmetry or higher (*e.g.*, an octahedron for $n = 3$), both achiral structures. For all other values of θ the two polygons have the chiral D_n symmetry. In terms of chirality measures, this means that the set of $2n$ equivalent atoms have zero CCM values for the rotation angles indicated and finite values for all other angles, whereupon one maximum CCM value should be expected between two successive achiral geometries, resulting in a dependence of the CCM on the rotation angle of the type shown in Fig. 7. We can recognize in the first portion of the general curve shown here (for angles between 0 and π/n) the pattern presented by the first shell of hexacoordinate complexes (Fig. 1). The fact that the maximum CCM value does not appear exactly halfway between the two achiral geometries arises because the CCM approach measures the distance to the closest achiral structure, not necessarily the prism or the antiprism, as discussed earlier for the case of the $[ML_6]$ complexes.

A molecule with only one pair of n-gons in an arbitrary chiral conformation with $\theta = \gamma$ can be converted into its mirror image by rotating the two polygons to $\theta = -\gamma$ or $\theta = 2\pi/n - \gamma$, thus passing through the $\theta = 0$ or $\theta = \pi/n$ achiral

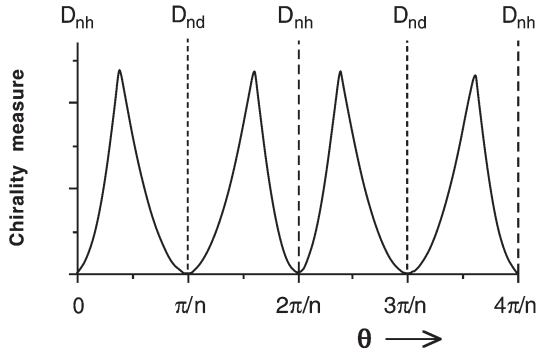

Fig. 7 CCM (arbitrary scale) of a set of $2n$ atoms with D_n symmetry as a function of the rotation angle θ between two n-gons.

geometries, respectively. In other words, such a molecule will undergo enantiomerization through an achiral path if the rotation axis is preserved. This simple symmetry analysis tells us that internal rotation enantiomerization paths in $[MX_6]$ complexes with monodentate ligands proceed per force through an achiral transition state. The same behavior should be expected for the enantiomerization of metaprismatic $[MX_8]$ compounds.

If we consider now molecules with more than one set of $2n$ equivalent atoms, enantiomerization of the molecule requires the enantiomerization of every set. Each set behaves in the same way just discussed, proceeding through an achiral path. However, the enantiomerization of the different sets may not be synchronous. If that is the case, when one set of atoms has reached the achiral intermediate geometry, other sets may be in a chiral situation, so that at every point along the path there are one or more chiral sets and the whole molecule is always chiral along the path. In short, asynchronous enantiomerization of the different sets of equivalent atoms results in a chiral enantiomerization path for such a molecule.

According to these ideas, we can identify different cases of enantiomerization reactions regarding the chirality of their transition states: (1) $[MX_6]$ complexes with monoatomic ligands, which proceed through an achiral enantiomerization path, since there is only one shell that must undergo enantiomerization. (2) $[M(SR)_6]$ complexes, which present two shells that enantiomerize in an asynchronous way, resulting in a chiral enantiomerization path. (3) [M(phenanthroline)$_3$] complexes with rigid bidentate ligands, which may undergo synchronous rotation of the first and successive shells and yield an achiral enantiomerization path. (4) Tetragonal propellers $[M(C_6Cl_5)_6]$, that preserve an achiral first shell throughout the enantiomerization pathway, but for which the second and third shells enantiomerize in a synchronous way leading therefore to an achiral path. Having discussed already in some detail the simplest case of complexes with monoatomic ligands, let us comment on specific examples of the remaining cases.

Compounds with two non-rigid enantiomeric shells

The most interesting case of enantiomerization through internal rotation is that found for homoleptic hexacoordinate compounds with two non-rigid shells, as found in the $[Zr(SR)_6]^{2-}$ complexes,[13] which present chiral metaprismatic structures. If we consider the simplest example of this family, that with R = H, we have two sets of $2n$ (n = 3) equivalent atoms and each of them must undergo enantiomerization to produce the enantiomerization of the whole molecule. But now the enantiomerization of the two sets cannot proceed independently because of the S–H bonds that hold them together. Hence, we need two parameters to describe the structure of our compound along the path (see **14** and **15**). The first one is the twist angle between two parallel faces of the coordination polyhedron formed by the sulfur atoms (θ in **14**). Since in this case clockwise and anticlockwise rotations are not equivalent due to the orientation of the thiolato substituents we will adopt the convention illustrated in **14** that negative angles correspond to anticlockwise rotations. The chirality of the first shell will be determined only by this angle. The second parameter that is needed describes the orientation of the substituents bonded to the sulfur atoms and a convenient choice is the c–M–S–R torsion angle (τ), whereby c is the centroid of the corresponding trigonal face as shown in **15**. What is interesting in this case is that the chirality of the second shell depends on the values of both parameters θ and τ and is therefore uncorrelated to that of the first shell, which depends only on θ. As a result, in the $[M(SR)_6]$ complexes S_1 and S_2 may vary independently, each shell can pass through achirality at different stages along the enantiomerization path and therefore the whole molecule may never become achiral.

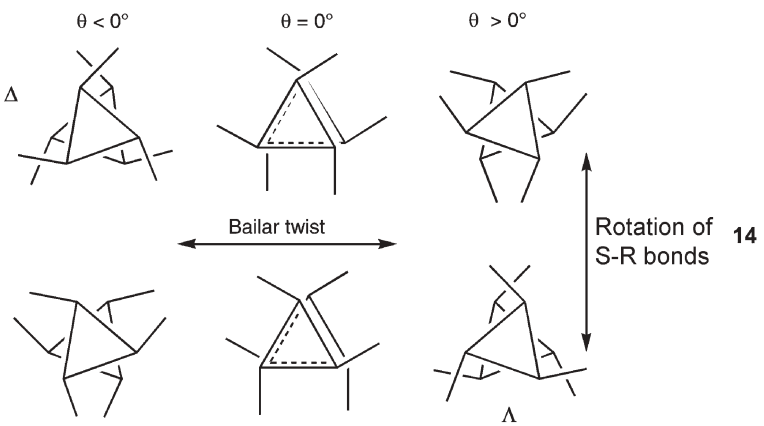

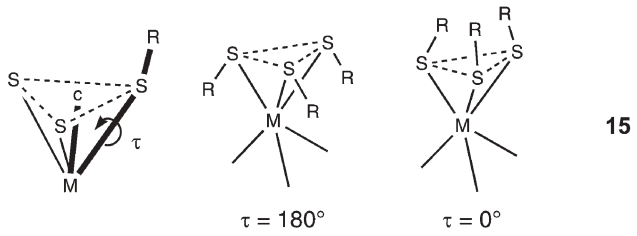

15

As shown in **14**, the rearrangement of the molecule leading from the Δ to the Λ enantiomer requires two geometrical changes: the Bailar twist of the first shell and the rotation of the S–R bonds around the Zr–S axes. Regarding the chirality of the enantiomerization pathway it is fundamental to know if these two movements occur in synchronous or asynchronous ways. To answer this question we must analyze the potential energy surface for each case since it will depend greatly on the nature of the R groups. As an example we show in Fig. 8 the energy surface calculated for a simple case,[13] that of $[Zr(SH)_6]^{2-}$. The energy and chirality values for some singular points of this surface are summarized in Table 1.

One should note that points X and Y of the energy surface correspond to an octahedral ($\theta = 60^\circ$ in Y) or trigonal prismatic first shell ($\theta = 0^\circ$ in X), with the second shell at $\tau = 180^\circ$ having the same conformation, *i.e.*, a trigonal antiprism in Y and trigonal prism in X. Furthermore, the points related by inversion through X or Y correspond to enantiomeric structures, whereas points separated by a 120° interval along the θ axis represent identical structures. Thus, points A and A′ in Fig. 8 correspond to the two enantiomeric structures of minimal energy and three different pathways connecting the minima can be found on the surface:

1) the least motion path A–L–A′ with a barrier of 19 kcal mol^{-1}

2) an automerization path connecting two equivalent A minima through point M with a similar barrier (16 kcal mol^{-1})

3) a long path with barriers of about 18 kcal mol^{-1} connecting A and A′ through points N–B–P–B′–N′. Of these points, N and P are transition states, while B is a minimum 10 kcal mol^{-1} above the global minimum.

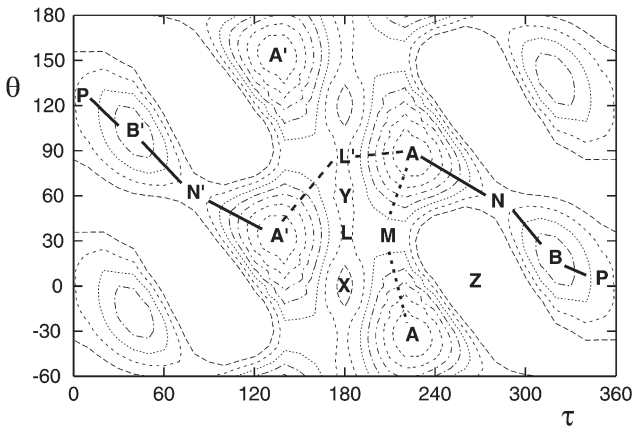

Fig. 8 Potential energy surface calculated for $[Zr(SH)_6]^{2-}$ as a function of the Bailar twist angle θ and the orientation of the S–H bonds, τ. Points **P**, **X** and **Y** correspond to achiral structures, other points labelled to chiral geometries. Isoenergy curves are plotted at 3 kcal mol^{-1} intervals. Reproduced with permission from ref. 13. Copyright (2003) Wiley-VCH.

Table 1 Position, relative energies (kcal mol^{-1}) and continuous chirality measures (CCM) of some relevant points of the potential energy surface of $[Zr(SH)_6]^{2-}$ (Fig. 8)

Point	Nature	θ	τ	CCM	Energy
A	minimum	−32	225	1.68	0
B	minimum	18	319	2.92	9.9
L	transition state	−35	180	3.57	18.7
M	transition state	30	211	1.48	16.3
N	transition state	60	280	3.88	19.3
P	transition state	0	360	0.00	18.2
X	maximum	0	180	0.00	22.5
Y	maximum	60	180	0.00	19.4
Z	maximum	10	260	1.85	43.3

It is interesting to see that the shortest path, A–L–A′, is a chiral path with a chiral transition state (see the CCM values in Table 1), while the longer path is achiral since it passes through the achiral transition state P. We note also that two enantiomeric transition states L and L′ exist for the chiral path.

Thus, contrary to the intuitive notion that interconversion of left- and right-handed enantiomers should proceed through an achiral structure, we find here that the most plausible path in this case has a chiral transition state. The reason for this can be easily understood. At the minimum, both the ZrS_6 and the H_6 shells are chiral, hence enantiomerization requires the generation of the mirror images of both groups. From the minimal energy geometry A to the transition state L, the twist angle of the ZrS_6 fragment changes little, its chirality is retained and its mirror image is generated only after the transition state. In contrast, the H_6 shell is nearly halfway along its reorientation motion at point L. In other words, the changes in chirality of the two shells proceed in an asynchronous way and hence the whole structure remains chiral along the whole path.

In order to solve the apparent contradiction of interconverting left- and right-handed enantiomers without passing through an achiral structure we must make a subtle distinction between chirality and handedness.[25] While the concept of chirality can be defined unambiguously (based on the non-superimposability of mirror images) the left or right labeling of chiral structures is known to be inherently problematic. In our case we have used only the handedness of the ZrS_6 core to label the enantiomers, but since the H_6 group is also chiral, for some structures the corresponding labels cannot be assigned, a problem of latent handedness that appears for any labeling procedure.[25]

Tris(chelate) complexes

A different situation is found for tris(chelate) complexes, for which the twist of the rigid ligands induces a synchronous rotation of the first and second shells, hence changes of chirality in both shells. As an illustration for this case let us analyze the enantiomerization of a $[M(phen)_3]^{2+}$ ion. Although different concerted rearrangement mechanisms have been proposed for the racemization of tris(chelate) complexes,[26,27] we will discuss here only the Bailar path in which the chelate is

twisted about its 3-fold symmetry axis to reach its enantiomer through a trigonal prismatic transition state (see **3**).

In this case it is convenient to describe the enantiomerization path using a single parameter, the twist angle of the rigid phenanthroline ligands with respect to the trigonal axis, φ. Thus, $\varphi = 0^\circ$ corresponds to the trigonal prismatic geometry depicted in **4** (left and center), $\varphi = 35^\circ$ represents the pseudo-octahedral situation of the MN_6 core with the parameters adopted here, and $\varphi = 90^\circ$ would correspond to the hypothetical situation in which the three ligands lie on the same plane, with the metal center in a hexagonal coordination. The evolution of the molecular chirality measure along the Bailar path (Fig. 9) that interconverts the Δ and the Λ enantiomers passes through a conformation with achiral trigonal prismatic geometry ($\varphi = 0^\circ$) and, consequently, we can conclude that this is an achiral enantiomerization path. Even if the motion of the whole phenanthroline ligands throughout the Bailar twist is correlated to the rotation of the first shell (N_6 atoms set), it is interesting to separately analyze the evolution of the chirality by shells. If we start with a pseudo-octahedral coordination of the first shell (Δ point in Fig. 9, with $S_1 = 0$) we see that moving from one enantiomer to the other results in an increase of the chirality of this shell that reaches a maximum at $\varphi \approx -18^\circ$, then the chirality decreases and reaches a zero value for the trigonal prismatic geometry ($\varphi = 0^\circ$), and the shape of the S_1 curve is mirrored for positive φ values, finally becoming achiral for the pseudo-octahedral coordination sphere Λ. As discussed above, in the pseudo-octahedral geometry the molecular chirality is associated with the second shell, as reflected by the non-zero value found for S_2, since the first shell is achiral. However, upon rotation the S_2 value decreases until the achiral trigonal prismatic geometry ($\varphi = 0^\circ$) is achieved, increasing again and finally reaching the isochiral geometry of the alternative enantiomer. In summary, the fact that the phenanthroline ligands are rigid and coplanar to the chelate ring results in a synchronous rotation of the first and successive shells in such a way that all the shells simultaneously form trigonal prisms at $\varphi = 0^\circ$ (*i.e.*, $\theta_i = 0^\circ$ for all shells *i*) and the internal rotation enantiomerization path is an achiral one.

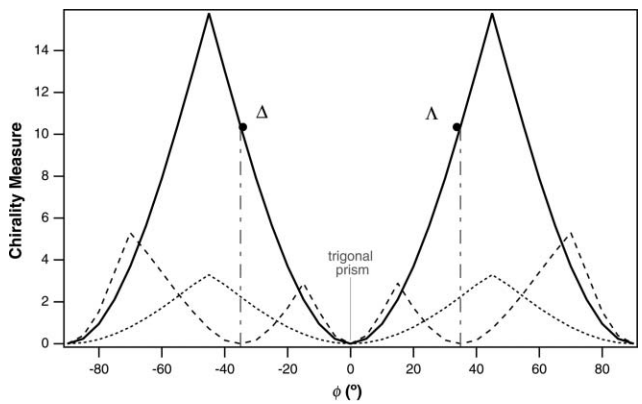

Fig. 9 Chirality measures for the complete structure (S_f, continuous line), for the first shell (S_1, dashed line) and for the second shell (S_2, dotted line) of a model $[M(phen)_3]^{2+}$ ion as a function of the angle between the phenanthroline ligands and the trigonal axis (φ).

Tetragonal propellers

For square planar complexes with ligands that present hindered rotation around the metal–ligand bonds, like the $[M(C_6Cl_5)_4]$ propeller, enantiomerization can be achieved through rotation of the C_6Cl_5 blades about the M–C bonds, as depicted in **8**. Throughout such a pathway, molecular chirality arises only from the second shell, since the first shell, MC_4 remains planar. If we start with the enantiomer A having $\tau = 30^\circ$, we can obtain its mirror image A′ by twisting the aryl groups either clockwise or anticlockwise. It is easy to convince ourselves that in this case the two possible enantiomerization paths involving the concerted twist of all four aryl groups will necessarily pass through an achiral conformation: that with the aryl groups perpendicular to the coordination plane ($\tau = 0^\circ$) or that with the four ligands lying on the plane ($\tau = 90^\circ$). This is nicely reflected in the evolution of the chirality measure with the rotation angle τ, shown in Fig. 10, where the maximum degree of chirality is reached at $\tau = 45^\circ$. However, since the accessibility of the alternative enantiomerization pathways is dictated by their relative energies, we can rule out the path that proceeds through a structure with four coplanar phenyl rings, since it implies a physically impossible situation in which the atoms on neighboring ligands would be superimposed. Related to this question, it is interesting to note that there are other geometries (points B and B′ in Fig. 10) with the same value of the chirality measure as our reference structure, *i.e.* there are four isochiral diastereomeric structures, grouped in two pairs of enantiomers: A and A′ are enantiomeric and have the same energy, whereas B and B′ are also mirror images of each other but have different energy than A and A′.

5. Molecular and supramolecular chirality

It is worth commenting here that ligands containing bipyridine or phenanthroline units are commonly used to form chiral helicates or trefoil knots, in which the helical wrapping of the ligands is the most obvious manifestation of the chirality of such fascinating molecules. Since the double stranded helicates are in fact formed by repetition of $M(bipy)_2$ units it is not surprising to find[15] (at least for relatively rigid bidentate ligands) that the chirality behavior of these building blocks is the same as that of the mononuclear analogues. This means

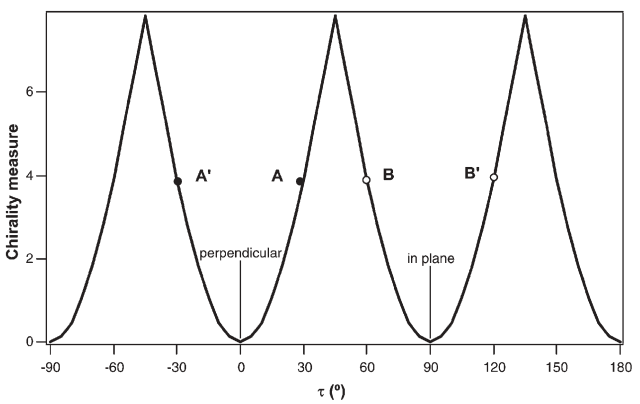

Fig. 10 Chirality measure of a $[M(C_6Cl_5)_4]$ propeller as a function of the rotation angle of the blades around the M–C bonds (see **8**).

that in double stranded helicates chirality is imprinted already at the core of the $M(N_2C_2)_2$ building block (the first two shells), and their helicity and chirality are intimately linked to the chirality of the metal coordination sphere. To illustrate this, we give in Table 2 the chirality measures of the fragments of the copper helicate **16**, shown in Fig. 11.[28]

It seems clear that the chirality content of that helical structure is already imprinted in the CuN_4 cores, while there is little chirality in each bipyridine chelating unit. The arrangement of two bipyridine units around each copper atom and the assembly of two such units in the full molecule have the effect of amplifying the chirality of the first coordination sphere. In that sense, we would say that these compounds present molecular chirality.

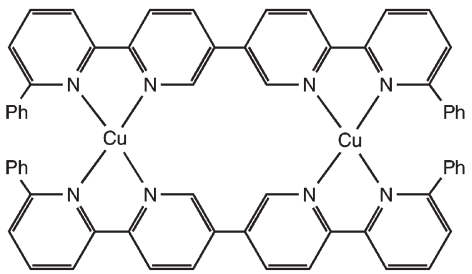

16

The main significant difference between helicates and mononuclear analogues is that the former appear concentrated near the tetrahedral end of the twist pathway, most probably a result of the usual choice of d^{10} ions such as Cu(I), Ag(I) or Zn(II) for the construction of double-stranded helicates. Thus, the possibility is open for other choices of building blocks for helicates, such as twisted square planar Pt(II) cores[29,30] which, nevertheless, have not been attempted so far.

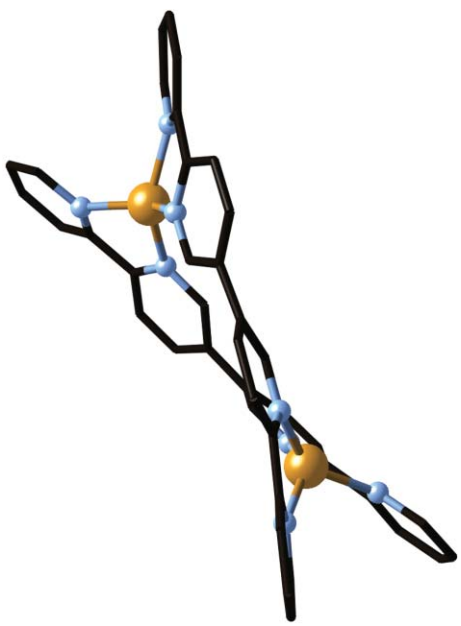

Fig. 11 Molecular structure of the skeleton of a Cu(II) helicate[28] formed by chemically linking two $Cu(bipy)_2$ units.

In contrast, one can build extended chiral structures from strictly achiral building units, hence the chirality should be considered in these cases strictly supramolecular. A few examples of very simple composition from the realm of transition metal chemistry are gathered in Table 3. We can see there that the MX_4 building blocks are achiral beyond chemical accuracy (0.01 units). However, the chirality measures of half helical turn (3 units for $CsCuCl_3$, AgF_3 and AuF_3, 4 units for $LiZnNbO_4$) or one full turn are comparable to that of the helicate discussed above. As an example, the beautiful chiral structure of AuF_3 is shown in Fig. 12.

Table 2 Chirality measures of several fragments of the Cu^I helicate **16**

One bis(bidentate) ligand	0.33
One CuN_4 core (average)	2.5
One $Cu(bipy)_4$ unit (average)	5.4
Full $Cu_2(bipy)_4$ helix (without pending Ph groups)	6.08

Table 3 Chirality measures of several fragments of helical structures, compared with those of the molecular helicate **16** (Table 2)

	Building block	Monomer	Half turn	Full turn
$CsCuCl_3$	square planar	0.01	6.38	6.29
AuF_3	square planar	0.00	6.46	5.52
AgF_3	square planar	0.00	3.17	6.12
$LiZnNbO_4$	octahedral	0.12	0.08	7.91
		CuN_4 shell	full molecule	
Helicate **16**		2.5	6.08	

Since the determination of the CCM relies on crystallographic data, we must recall that in the case of chiral molecules, there are two options as to the space group of the crystal: An enantiomorphic space group, that packs the molecules in a homochiral way, and a non-enantiomorphic group, which brings about the packing of pairs of enantiomers and results in an achiral compound.[31] Also, a recent discussion on the construction of supramolecular chiral species with chiral or achiral building blocks can be found in the literature.[32]

6. Chirality in spin crossover systems

A very interesting situation can be found in hexacoordinate spin-crossover complexes with bidentate ligands. In those systems, the high spin configuration occurring at high temperature presents longer metal–ligand bond distances than the low spin configuration that becomes the most stable one at low temperatures. Such a structural effect, due to the different occupation of the σ^*(M–L) molecular orbitals (of e_g symmetry in the octahedron), has been quantified in a number of cases from X-ray diffraction structural determinations at variable temperature. A longer M–L bond distance for rigid bidentate ligands implies a smaller normalized bite b (**11**) and, since a smaller bite results in a larger trigonal twist toward the trigonal prism, the transition from high-spin to low spin configuration upon temperature lowering produces a significant amount of Bailar rotation, hence a significant quantitative variation in molecular chirality.

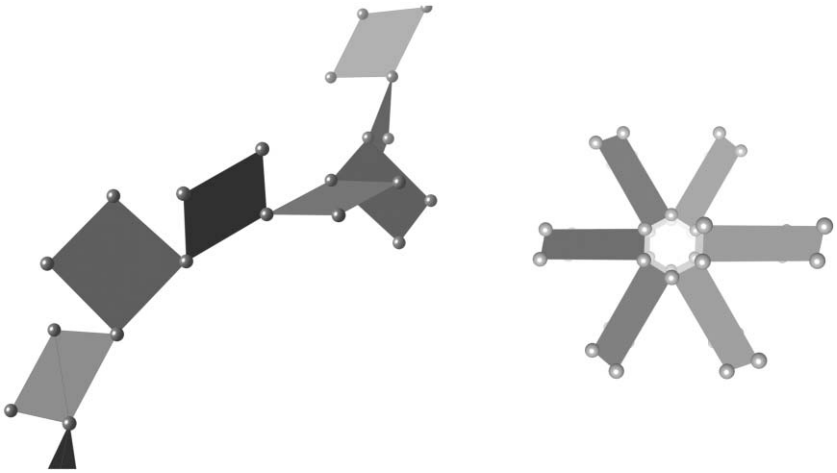

Fig. 12 Helical structure of the AuF_3 chains (left) and projection along its 6_1 screw axis (right).

There are several consequences of the relationship between spin crossover and quantitative chirality.[5] (a) A strong dependence of chirality on temperature appears (see Fig. 13 for an example). (b) Chirality and magnetic moment are correlated in these systems, both increasing or decreasing simultaneously (see Fig. 14). (c) The rates of racemization reactions proceeding through a Bailar twist should present a stronger temperature dependence in spin crossover systems than in analogous complexes with only one thermally accessible spin configuration.

7. Concluding remarks

The continuous chirality measures, as applied to experimental or theoretical structural data, provide a useful quantitative description of molecular chirality and we propose that its application to the stereochemical analysis of transition metal compounds should become a standard protocol. Measurement of chirality at the submolecular level is also interesting, since the properties associated to chirality, such as circular dichroism and enantioselective catalysis, depend on the stereochemistry of the molecular fragment associated with electronic transitions and with the catalytically active site, respectively. The concept of chirality amplification or attenuation by ligands probably deserve some thought when designing new asymmetric molecules, specially in regard with their enantiocatalytic properties. Our shell analysis of molecular chirality shows that one can establish a general pattern for chirality contents of families of complexes with very different substituents at the outer shells. From the mechanistic viewpoint, the analysis of shell chirality could be useful to predict whether an enantiomerization pathway should be expected to proceed through a chiral or an achiral transition state.

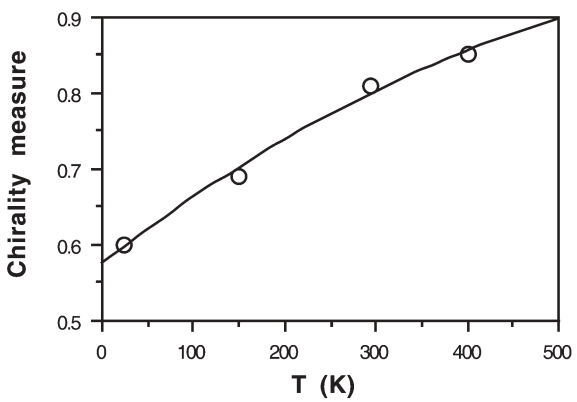

Fig. 13 Temperature dependence of the chirality measure of the FeS_6 core in the spin crossover dithiocarbamato complex $[Fe(Me_2dtc)_3]$. Adapted with permission from ref. 5. Copyright (2003) American Chemical Society.

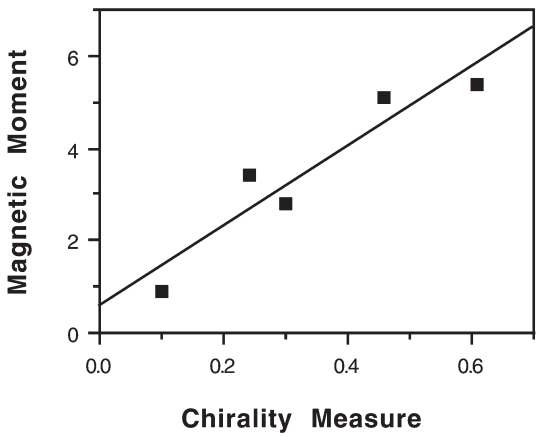

Fig. 14 Correlation between chirality measure of the $Fe^{III}S_6$ core and the magnetic moment (in Bohr magnetons) for spin crossover dithiocarbamato complexes. Adapted with permission from ref. 5. Copyright (2003) American Chemical Society.

Acknowledgements

This work has been supported by Dirección General de Enseñanza Superior (DGES), project PB98-1166-C02-01, and Comissió Interdepartamental de Ciència i Tecnologia (CIRIT), grant SGR99-0046. D. A. acknowledges support from the Israel Science Foundation (Grant 30/01).

Readers who would like to test and use our programs are encouraged to contact us at david@chem.ch.huji.ac.il

Santiago Alvarez,*[a] Pere Alemany[b] and David Avnir*[c]
[a]*Departament de Química Inorgànica, Universitat de Barcelona, Diagonal 647, 08028 Barcelona, Spain. E-mail: santiago@qi.ub.es*
[b]*Departament de Química Física and Centre de Recerca en Química Teòrica, Universitat de Barcelona, Diagonal 647, 08028 Barcelona, Spain. E-mail: pere@qf.ub.es*
[c]*Institute of Chemistry and The Lise Meitner Minerva Center for Computational Quantum Chemistry, The Hebrew University of Jerusalem, Jerusalem 91904, Israel. E-mail: david@chem.ch.huji.ac.il*

References

1 M. Petitjean, *Entropy*, 2003, **5**, 271.
2 D. Avnir, H. Zabrodsky Hel-Or and P. G. Mezey, in *'Encylopedia of Computational Chemistry'*, ed. P. von Rague Schleyer, Chichester, 1998.
3 H. Zabrodsky, S. Peleg and D. Avnir, *J. Am. Chem. Soc.*, 1992, **114**, 7843.
4 D. Yogev-Einot and D. Avnir, *Acta Crystallogr, Sect. B: Struct. Sci.*, 2004, **60**, 163.
5 S. Alvarez, *J. Am. Chem. Soc.*, 2003, **125**, 6795.
6 M. Pinsky, K. B. Lipkowitz and D. Avnir, *J. Math. Chem.*, 2001, **30**, 109.
7 H. Zabrodsky and D. Avnir, *J. Am. Chem. Soc.*, 1995, **117**, 462.
8 M. Pinsky and D. Avnir, *Inorg. Chem.*, 1998, **37**, 5575.
9 O. Katznelson, J. Edelstein and D. Avnir, *Tetrahedron: Asymmetry*, 2000, **11**, 2695.
10 L. Bellarosa and F. Zerbetto, *J. Am. Chem. Soc.*, 2003, **125**, 1975.
11 S. Alvarez, M. Pinsky and D. Avnir, *Eur. J. Inorg. Chem.*, 2001, 1499.
12 J. C. Friese, A. Krol, C. Puke, K. Kirschbaum and D. M. Giolando, *Inorg. Chem.*, 2000, **39**, 1496.
13 P. Alemany, S. Alvarez and D. Avnir, *Chem. Eur. J.*, 2003, **9**, 1952.
14 S. Alvarez, M. Pinsky, M. Llunell and D. Avnir, *Crystallogr. Eng.*, 2001, **4**, 179.
15 S. Alvarez and D. Avnir, *Dalton Trans.*, 2003, 562.
16 D. Casanova, J. Cirera, M. Llunell, P. Alemany, D. Avnir and S. Alvarez, *J. Am. Chem. Soc.*, 2004, **126**, 1755.
17 D. Casanova, M. Llunell, P. Alemany and S. Alvarez, *Chem. Eur. J.*, 2005, DOI: 10.1002/chem.200400799.
18 P. J. Alonso, J. Forniés, M. A. García-Monforte, A. Martín, B. Menjón and C. Rillo, *Chem. Eur. J.*, 2002, **8**, 4056.
19 D. L. Kepert, *'Inorganic Stereochemistry'*, Springer Verlag, Berlin, 1982.
20 S. Alvarez, D. Avnir, M. Llunell and M. Pinsky, *New J. Chem.*, 2002, **26**, 996.
21 K. B. Lipkowitz, S. Schefzick and D. Avnir, *J. Am. Chem. Soc.*, 2001, **123**, 6710.
22 S. Alvarez, S. Schefzick, D. Avnir and K. B. Lipkowitz, *Chem. Eur. J.*, 2003, **9**, 5832.
23 K. Mislow, *'Introduction to Stereochemistry'*, Benjamin/Cummings, 1965. Reprinted by Dover Publications, Mineola, NY, 2002.
24 R. D. Peacock and B. Stewart, in *'Comprehensive Coordination Chemistry II'*, ed. J. A. McCleverty and T. J. Meyer, Pergamon, Oxford, 2004.
25 Y. Pinto and D. Avnir, *Enantiomer*, 2001, **6**, 211.
26 A. Rodger and B. F. G. Johnson, *Inorg. Chem.*, 1988, **27**, 3062.
27 A. von Zelewsky, *'Stereochemistry of Coordination Compounds'*, J. Wiley, 1996.
28 P. N. W. Baxter, J.-M. Lehn and K. Rissaren, *Chem. Commun.*, 1997, 1323.
29 A. von Zelewsky, *Coord. Chem. Rev.*, 1999, **101**, 3457.
30 C. Deuschel-Cornioley, H. Stoeckli-Evans and A. von Zelewsky, *J. Chem. Soc., Chem. Commun.*, 1990, 121.
31 J. P. Glusker, M. Lewis and M. Rossi, *'Crystal Structure Analysis for Chemists and Biologists'*, VCH, New York, 1994.
32 M. Ziegler, A. V. Davis, D. W. Johnson and K. N. Raymond, *Angew. Chem. Int. Ed.*, 2003, **42**, 665.

